Calibration of a Polarimetric Imaging SAR

Kamal Sarabandi, *Member, IEEE*, Leland E. Pierce, *Member, IEEE*, and Fawwaz T. Ulaby, *Fellow, IEEE*

Abstract— **Calibration of polarimetric imaging SAR's using point calibration targets is discussed in this paper. The four-port network calibration technique [5] is used to describe the radar error model. The processor ambiguity function and the radar distortion matrices are then combined to form a generalized polarimetric ambiguity function. The polarimetric ambiguity function of the SAR is then found using a single point target, namely a trihedral corner reflector. Based on the resultant polarimetric ambiguity function, an estimate for the backscattering coefficient of the terrain is found using a modified version of the STCT technique [5]. A radar image recorded by the JPL aircraft SAR, which includes a variety of point targets, is used for verification of the new calibration method. The calibrated responses of the point targets are compared both with theory and responses based on the POLCAL technique [8]. Also, using a uniform area of the imaged scene, responses of a distributed target are compared using the modified STCT and POLCAL techniques.**

I. Introduction

Accurate knowledge of the scattering matrix of a target is an important ingredient toward extracting biophysical information about the target. The scattering matrix of a target can be measured by using a set of orthogonal polarizations. In practice, however, it is very difficult, if not impossible, to design an antenna system with perfect isolation between the orthogonal polarization channels, which leads to contamination of the measurements.

In recent years, considerable effort has been devoted to the development of techniques for calibrating polarimetric radar systems. Calibration techniques available in the literature can be categorized into two major groups: 1) calibration techniques for imaging radars, and 2) calibration techniques for point-target measurement systems, which may also be appropriate for imaging radars. In the first group, the scattering properties of clutter are usually employed to simplify the calibration problem [6]. van Zyl [8] and Klein [3] developed a method for estimating the cross-talk contamination of the antenna by assuming that the co- and cross-polarized responses of natural targets with azimuthal symmetry are uncorrelated. Among the point-target calibration techniques, the generalized calibration technique by Whitt *et al.* [10] characterizes the distortion matrices of the receive and transmit antenna by using three calibration targets. In a similar technique by Barnes [1] the distortion matrices are obtained by using targets with specific scattering matrices. Although, in principle, these techniques can fully characterize the distortion matrices, they are very sensitive to target alignment and to precise knowledge of the theoretical values of the scattering matrices of the calibration targets. A third calibration technique for point targets by Sarabandi *et al.* [4] uses a sphere and any other depolarizing calibration target (scattering matrix of this target need not be known), and is therefore immune to errors caused by target orientation and lack of precise knowledge of the theoretical values of the calibration targets' scattering matrices. However, the drawback of this method is that it does not account for cross-talk contamination in the antenna. The isolated antenna assumption can lead to significant errors in the cross-polarized terms when the ratio of cross- to like-polarized terms is small and/or cross-talk contamination is large. To remove this drawback while maintaining insensitivity to orientation of the calibration target, a single target calibration technique (STCT) was recently developed [5].

The main thrust of this paper is to show how the point target calibration techniques can be applied to imaging SAR's. In particular, the STCT will be employed here since it only requires one calibration target. Hence, problems associated with the relative positions of point targets with respect to the center of the imaged pixels can be avoided. This will be explained further in Section II. This method is then compared with the POLCAL technique [8], which was developed specifically for imaging radars.

Manuscript received February 6, 1991; revised December 5, 1991. This project was conducted under JPL Contract #JPL-C-958 749.

The authors are with the Radiation Laboratory, Department of Electrical Engineering and Computer Science, University of Michigan, Ann Arbor, MI 48109-2122.

IEEE Log Number 9107524.

II. A New Approach for Calibration of Imaging SAR's

In this section, we introduce a method for calibrating polarimetric imaging SAR's which requires a single point target. In this method, the polarimetric ambiguity function of the SAR processor as well as the distortion matrices of the radar system are found from the measured response due to the presence of a trihedral corner reflector. First, a summary of the single target calibration technique (STCT) is given and then a theoretical model which relates the point target response to distributed targets will be developed. The model, in conjunction with the STCT, is then used to obtain an approximate calibration matrix, which is used to compute the backscattering coefficient of any pixel.

A. Single Target Calibration Technique

A salient feature of the STCT is that it is convenient to use under field conditions. The advantages of this technique over the other techniques are that (1) the calibration is immune to errors caused by uncertainties in the relative orientation of calibration targets and (2) fewer calibration targets are required to be deployed. As will be shown later, SAR calibration techniques that require more than one calibration target face a number of target positioning problems. That is, unless the

calibration targets are in the same relative location within their respective pixels, they would usually exhibit different responses. The single target calibration technique (STCT) has been tested both under laboratory and field conditions using *L*-, *C*-, and *X*-band scatterometer systems and it has been shown that a calibration accuracy of 0.5 dB in amplitude and 5° in phase can be achieved.

This section provides a summary of the STCT formulation and associated assumptions and approximations. In this technique, the antenna system and two orthogonal directions in free space are modeled as a four-port passive device. Using the reciprocity property of the four-port network, the range gating capability of the radar system, and the scattering matrix of the target, the incident and returned signals are related by a two-port matrix representation. Excluding the propagation phase and amplitude factor, the measured scattering matrix of a target with real scattering matrix $\boldsymbol{S}$ is given by [5]

$$\begin{aligned}\boldsymbol{U} &= \boldsymbol{RST} \\ &= \begin{bmatrix} R_v & C_1R_v \\ C_2R_h & R_h \end{bmatrix} \boldsymbol{S} \begin{bmatrix} T_v & C_2T_h \\ C_1T_v & T_h \end{bmatrix}. \end{aligned} \tag{1}$$

The complex quantities R_p, T_q are the receive and transmit channel distortions with $p, q = v, h$ and $C_{1,2}$ are the antenna cross-talk factors. Equation (1) can be further simplified by assuming that the horizontal and vertical radiating elements of the antenna system are similar, hence $C_1 = C_2 = C$. Although (1) has been derived for single-antenna radars, it is still valid for antennas composed of many active elements as long as the elements are identical. Once the distortion parameters of the radar system are found, the actual scattering matrix of the target can be obtained from

$$\boldsymbol{S} = \frac{1}{R_vT_v(1+C^2)^2} \begin{bmatrix} 1 & -C\frac{R_v}{R_h} \\ -C & \frac{R_v}{R_h} \end{bmatrix} \boldsymbol{U} \begin{bmatrix} 1 & -C \\ -C\frac{T_v}{T_h} & \frac{T_v}{T_h} \end{bmatrix}. \tag{2}$$

The distortion parameters can be obtained by measuring a trihedral corner reflector with radar cross section σ_t whose scattering matrix is diagonal. Suppose the measured scattering matrix of the trihedral is denoted by $\boldsymbol{U}_t$, then it can be shown that the antenna cross-talk factor is obtained from

$$C = \pm\frac{1}{\sqrt{a}}(1 - \sqrt{1-a}) \tag{3}$$

To meet the condition $|C| < 1$, the branch cut for $\sqrt{1-a}$ is chosen such that $\mathrm{Re}[\sqrt{1-a}] > 0$. Therefore, C is determined from the trihedral measurement within a $\pm$ sign. In (3), the complex quantity a is related to the trihedral measurement by

$$a \triangleq \frac{u^t_{vh}u^t_{hv}}{u^t_{vv}u^t_{hh}}.$$

The expression for channel imbalances as required by (2) can also be obtained from the trihedral response as follows

$$R_vT_v = \frac{u^t_{vv}}{(1+C^2)\sqrt{\sigma_t/4\pi}} \tag{4}$$

$$\frac{R_v}{R_h} = \frac{1+C^2}{2C} \cdot \frac{u^t_{vh}}{u^t_{hh}} \tag{5}$$

$$\frac{T_v}{T_h} = \frac{2C}{1+C^2} \cdot \frac{u^t_{vv}}{u^t_{vh}}. \tag{6}$$

Although (1) and the STCT are based on several assumptions it will be shown that applying STCT as is developed in the coming sections significantly improves the channel isolation, channel amplitude balance, and the phase balance of the the JPL AirSAR data.

B. Modified STCT for Imaging Radars

Calibration techniques developed for point targets cannot be applied directly to distributed targets in imaging radars. The quantity of interest in imaging radars is the backscattering coefficient (σ^0) of the distributed targets as opposed to the radar cross section for point targets in nonimaging radars. External calibration usually requires measurement of targets with known scattering parameters. For imaging radars, no distributed calibration targets are available and therefore distortion parameters must be inferred from measurements of point calibration targets.

To understand the intermediate steps involved in calibration of imaging SAR's using point calibration targets, the process of generating a high resolution image from raw data must first be examined. The received raw data in each of the channels of a polarimetric SAR can be described by

$$U_{pq}(t) = \int_A S^0_{pq}(x', y')G\left(t - \frac{2R}{c}\right)dx'dy\, p, q = v, h \tag{7}$$

where A is the area illuminated by the physical antenna, $S^0_{pq}(x', y')$ is the reflectivity of the terrain being mapped, and p and q are the polarization state of the receiver and transmitter, respectively. Function $G(t)$ is a particular wave form radiated by the transmitter and can usually be represented by

$$G(t) = g(t)e^{i\omega_0 t} \tag{8}$$

where $g(t)$ is a slowly varying function and ω_0 is the angular carrier frequency of the radar system. In (7) R is the distance from the antenna to the scattering point (x', y') on the ground. This equation shows that the received signal is the superposition of the response from a large number of scatterers both within the illuminated area and within the time span that all echoes arrive simultaneously at the radar antenna.

In an imaging radar, the processor performs an operation on the received signal $U_{pq}(t)$ to retrieve the reflectivity of the scene, $S^0_{pq}(x, y)$. One such operation is to pass the signal through a matched filter having an impulse response $G^*\left(t - \frac{2R}{c}\right)$ [2], leading to an output

$$\begin{aligned} U'_{pq}(x, y) = \int_t \int_A S^0_{pq}(x', y')G\left(t - \frac{2R'}{c}\right) \\ \cdot G^*\left(t - \frac{2R}{c}\right)dx'dy'dt. \end{aligned} \tag{9}$$

By performing the integration with respect to time, the quantity

$$\psi(x, y; x', y') = \int_t G\left(t - \frac{2R'}{c}\right)G^*\left(t - \frac{2R}{c}\right)dt \tag{10}$$

known as the ambiguity function can be obtained. Therefore (9) can be written as

$$U'_{pq}(x, y) = \int_A S^0_{pq}(x', y')\psi(x, y; x', y')dx'dy'. \tag{11}$$

If the ambiguity function is a Dirac delta function, i.e. $\psi(x,y;x',y') = \delta(x-x',y-y')$, the reflectivity function can be obtained from (11) directly. In practice, however, it is not possible to generate a Delta function for the ambiguity function because it would require infinite bandwidth and integration time.

By substituting (8) into (10) and assuming that $g(t)$ is a linearly frequency modulated pulse of duration $\tau\left(g(t) = e^{i\frac{\pi\Delta f}{\tau}t^2}\right)$ and that the integration time in (10) is over $N+1$ pulses of the transmitter we have

$$\psi(x,y;x',y') = \sum_{-\frac{N}{2}}^{\frac{N}{2}} e^{-2iw_0(R-R')/c} \int_{-\tau/2}^{\tau/2} e^{i\frac{\pi\Delta f}{\tau}\left[\left(t-\frac{2R'}{C}\right)^2-\left(t-\frac{2R}{C}\right)^2\right]}dt. \quad (12)$$

In (12), the ambiguity function is a smooth function with a peak at $x = x', y = y'$ which drops rapidly for values of (x',y') away from the peak. The first term in (12) gives the azimuthal resolution whereas the second term gives the range resolution of the SAR. Using (12) in (11) does not resolve $S^0_{pq}(x,y)$ completely and the measured quantity $U'_{pq}(x,y)$ contains backscattered energy from adjacent pixels. To obtain a better estimate of the backscattering coefficient a deconvolution process must be attempted, provided the ambiguity function is known.

Although the ambiguity function can be calculated in a manner similar to that outlined in connection with equation (12), in practice this approximation may not be accurate enough for calibration. In the derivation of (12), the antenna gain pattern has been ignored in (7), and for focused SAR's weighting factors must be used in (12). Also, for polarimetric SAR's the channel imbalances and antenna cross coupling factors introduce errors into the ambiguity function. Hence it is necessary that the ambiguity function be determined directly from the calibration process. Thus the ambiguity function of each channel for a polarimetric SAR may be different when the corresponding antenna patterns are different.

C. Calibration Procedure and Estimation of Backscattering Coefficient

One way of calibrating an imaging SAR using a point calibration target is by degrading the resolution of the image (while simultaneously decreasing the number of pixels) so that the point target response occupies only one pixel. In this case the calibration procedure would be identical to that of nonimaging radars. For example STCT can be applied directly as outlined in the previous section. There are two problems with this approach. The first is that the image quality is degraded, and the second is that the signal-to-background ratio for the calibration target is decreased. This approach is, therefore, not of interest and will not be followed any further.

The error model for a polarimetric SAR must include uncertainties caused by antenna cross talk and channel imbalances as well as the uncertainties in the ambiguity function. Suppose the radar system is linear. Since passing the received signal through a matched filter is also a linear process, the polarimetric response of the terrain with polarimetric reflectivity $\boldsymbol{S}^0(x,y)$ is given by

$$\boldsymbol{U}(x,y) = \boldsymbol{R}\left[\int_A \boldsymbol{S}^0(x',y')\psi(x,y;x',y')dx'dy'\right]\boldsymbol{T}. \quad (13)$$

In (13) the amplitude and phase of the propagation factor $\left(\frac{e^{2ik_0R}}{R^2}\right)$ has been excluded and $\boldsymbol{R}$ and $\boldsymbol{T}$ are, respectively, the receive and transmit distortion matrices. For a given range centered over a finite extent in the range direction, it is assumed that the distortion matrices and the ambiguity function are not a function of range and that the ambiguity function is not a function of absolute position, i.e.

$$\psi(x,y;x',y') = \psi(x-x',y-y').$$

Since radar images are discretized into a finite number of pixels, the discrete form of (13) must be considered, where the integral is approximated by a double summation; thus

$$\boldsymbol{U}(m,n) = \boldsymbol{R}\left[\sum_i\sum_j \boldsymbol{S}^0(i,j)\psi(m-i,n-j)\Delta x\Delta y\right]\boldsymbol{T}. \quad (14)$$

By changing the indexes of the summations such that the maximum of the ambiguity function occurs at $(0,0)$, (14) becomes

$$\boldsymbol{U}(m,n) = \boldsymbol{R}\left[\sum_i\sum_j \boldsymbol{S}^0(m-i,n-j)\psi(i,j)\Delta x\Delta y\right]\boldsymbol{T}. \quad (15)$$

In practice the indexes should be extended to values such that $|\psi(i,j)|$ is greater than some threshold above the noise level. Since both the ambiguity function and the distortion matrices are unknowns we may lump them together and, therefore, (15) takes the following form

$$\boldsymbol{U}(m,n) = \Delta x\Delta y \sum_{i=\frac{-N}{2}}^{\frac{N}{2}}\sum_{j=\frac{-M}{2}}^{\frac{M}{2}} \boldsymbol{\mathcal{R}}_{ij}\boldsymbol{S}^0(m-i,n-j)\boldsymbol{\mathcal{T}}_{ij} \quad (16)$$

where $\boldsymbol{\mathcal{R}}_{ij}$ and $\boldsymbol{\mathcal{T}}_{ij}$ are now called the receive and transmit ambiguity-distortion matrices, respectively. The error model given by (16) has the most general form, since it can include cases where the ambiguity function is different for different channels of the polarimetric SAR.

As was mentioned earlier, if the ambiguity function is a delta function, the reflectivity function can be obtained directly. On the other hand, if the reflectivity function is a delta function, then the functional form of the ambiguity function can be obtained. The reflectivity function of a point target is a delta function. For example, if a trihedral with radar cross section σ_T located at (x_0,y_0) is used as a calibration target, its reflectivity function is expressed by

$$\boldsymbol{S}^0_T(x,y) = \sqrt{\frac{\sigma_T}{4\pi}}\,\boldsymbol{I}\,\delta(x-x_0)\delta(y-y_0) \quad (17)$$

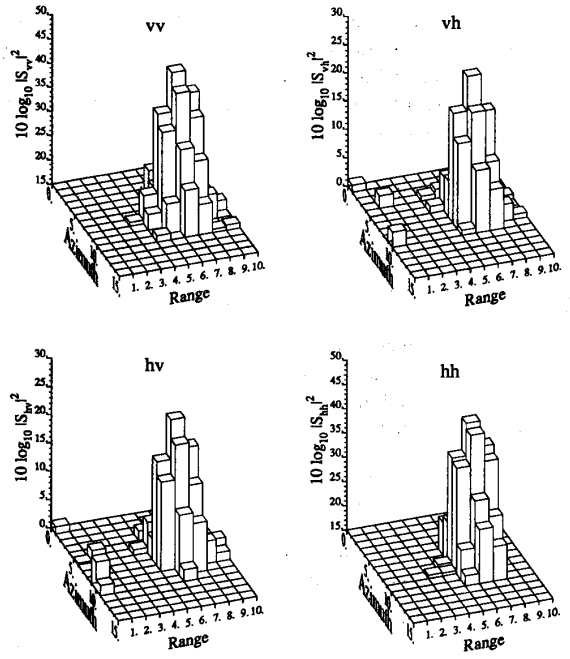

Fig. 1. Measured Ambiguity-Distortion Matrix values in dB for a single trihedral at L-band (1.25 GHz). A small region surrounding the brightest pixel is shown. The minimum value shown is the approximate noise (clutter) floor. Note the different vertical scales used for the copol and cross-pol figures.

where $\boldsymbol{I}$ is a 2×2 identity matrix. Substituting (17) into (13) results in the polarimetric response of the SAR to the trihedral. The discretized form of this response for a trihedral located at the klth pixel is given by

$$\boldsymbol{U}_T(m,n) = \sqrt{\frac{\sigma_T}{4\pi}}\,\boldsymbol{R}\,\boldsymbol{I}\,\psi(m-k,n-l)\,\boldsymbol{T}. \tag{18}$$

Changing the indexes in (18) such that $i = m - k$ and $j = n - l$ and then combining the resultant ambiguity function and distortion matrices, (18) becomes

$$\boldsymbol{U}_T(k+i,l+j) = \sqrt{\frac{\sigma_T}{4\pi}}\,\boldsymbol{\mathcal{R}}_{ij}\boldsymbol{I}\boldsymbol{\mathcal{T}}_{ij} \tag{19}$$

with

$$i \in \left\{-\frac{N}{2},\cdots,\frac{N}{2}\right\} \text{ and } j \in \left\{-\frac{M}{2},\cdots,\frac{M}{2}\right\}.$$

In deriving (19) we have assumed that the contribution from the background is negligible. In practice the point target must be located in a very smooth and uniform area such that the radar cross section is at least 30 dB above the clutter. Fig. 1 shows the measured amplitude of the polarimetric response of the JPL aircraft SAR to an 8-ft trihedral at L-band (1.25 GHz).

To obtain the ambiguity-distortion parameters, we notice that (19) provides $(M+1)\times(N+1)$ matrix equations similar to the matrix equation encountered in the single target calibration technique. Once the ambiguity-distortion parameters from the trihedral response are found, they can be used in (16), where the only unknown will be the reflectivity $\left(\boldsymbol{S}^0(m,n)\right)$ of the terrain. The expression given by (16) has a matrix convolution form that is extremely difficult, if not impossible, to invert in an exact form. However, an approximate form for the polarimetric reflectivity of the terrain $\left(\hat{\boldsymbol{S}}^0(m,n)\right)$ can be obtained. In this approximation it is assumed that over the pixels where the ambiguity function is nonzero the reflectivity of the terrain is constant and is equal to that of the center pixel (the pixel for which the ambiguity function is maximum). This approximation has a smoothing effect on the actual reflectivity function.

Under the mentioned approximation, (16) becomes

$$\boldsymbol{U}(m,n) = \Delta x \Delta y \sum_{i=\frac{-N}{2}}^{\frac{N}{2}} \sum_{j=\frac{-M}{2}}^{\frac{M}{2}} \boldsymbol{\mathcal{R}}_{ij}\hat{\boldsymbol{S}}^0(m,n)\boldsymbol{\mathcal{T}}_{ij}. \tag{20}$$

These matrices in the right-hand and left-hand side of (20) can be represented by vectors with four components. If the four-vector form of $\boldsymbol{U}(m,n)$ and $\hat{\boldsymbol{S}}^0(m,n)$ are, respectively, denoted by

$$\boldsymbol{\mathcal{U}}(m,n) = \begin{bmatrix} U_{vv}(m,n) \\ U_{vh}(m,n) \\ U_{hv}(m,n) \\ U_{hh}(m,n) \end{bmatrix}, \hat{\boldsymbol{\mathcal{S}}}^0(m,n) = \begin{bmatrix} \hat{S}^0_{vv}(m,n) \\ \hat{S}^0_{vh}(m,n) \\ \hat{S}^0_{hv}(m,n) \\ \hat{S}^0_{hh}(m,n) \end{bmatrix}$$

then

$$\boldsymbol{\mathcal{U}}(m,n) = \left[\sum_{i=\frac{-N}{2}}^{\frac{N}{2}} \sum_{j=\frac{-M}{2}}^{\frac{M}{2}} \boldsymbol{D}_{ij}\right] \hat{\boldsymbol{\mathcal{S}}}^0(m,n). \tag{21}$$

Matrix $\boldsymbol{D}_{ij}$ is a 4×4 matrix whose entries in terms of the entries of the ambiguity-distortion matrices are given by

$$\boldsymbol{D}_{ij} = \Delta x \Delta y \begin{bmatrix} \mathcal{R}^{ij}_{vv}\mathcal{T}^{ij}_{vv} & \mathcal{R}^{ij}_{vv}\mathcal{T}^{ij}_{hv} & \mathcal{R}^{ij}_{vh}\mathcal{T}^{ij}_{vv} & \mathcal{R}^{ij}_{vh}\mathcal{T}^{ij}_{hv} \\ \mathcal{R}^{ij}_{vv}\mathcal{T}^{ij}_{vh} & \mathcal{R}^{ij}_{vv}\mathcal{T}^{ij}_{hh} & \mathcal{R}^{ij}_{vh}\mathcal{T}^{ij}_{vh} & \mathcal{R}^{ij}_{vh}\mathcal{T}^{ij}_{hh} \\ \mathcal{R}^{ij}_{hv}\mathcal{T}^{ij}_{vv} & \mathcal{R}^{ij}_{hv}\mathcal{T}^{ij}_{hv} & \mathcal{R}^{ij}_{hh}\mathcal{T}^{ij}_{vv} & \mathcal{R}^{ij}_{hh}\mathcal{T}^{ij}_{hv} \\ \mathcal{R}^{ij}_{hv}\mathcal{T}^{ij}_{vh} & \mathcal{R}^{ij}_{hv}\mathcal{T}^{ij}_{hh} & \mathcal{R}^{ij}_{hh}\mathcal{T}^{ij}_{vh} & \mathcal{R}^{ij}_{hh}\mathcal{T}^{ij}_{hh} \end{bmatrix}.$$

Therefore, the calibrated estimate of the reflectivity matrix is given by

$$\hat{\boldsymbol{\mathcal{S}}}^0(m,n) = \boldsymbol{D}^{-1}\boldsymbol{\mathcal{U}}(m,n)$$

where

$$\boldsymbol{D} = \sum_{i=\frac{-N}{2}}^{\frac{N}{2}} \sum_{j=\frac{-M}{2}}^{\frac{M}{2}} \boldsymbol{D}_{ij}$$

is the calibration matrix, which is independent of pixel coordinates m and n. In practice, M and N are chosen so that most of the target response is included, typically a 5 pixel by 5 pixel region surrounding the brightest pixel. Gray *et al.* [12] perform a similar addition for calibration with point targets, but they are summing power data, whereas here we are dealing with complex data. Hence, it was felt that in our algorithm we should account for the relative phases of these pixels, as is done above.

It is worth mentioning that since the antenna patterns and the cross-talk factors are functions of range, the ambiguity function and thus the calibration matrix are functions of range also. Hence, in order to calibrate the image accurately it is necessary for an array of trihedrals to be deployed across the swath range.

III. JPL POLCAL Technique

A widely used method within the remote sensing scientific community for calibrating polarimetric imaging SAR's is the one developed at JPL known as POLCAL. This method is a combination of phase calibration by Zebker and Lou [11] and a calibration algorithm by van Zyl [8] based on properties of distributed targets. A summary of this technique is given below for comparison with the modified STCT method described in the previous section. A detailed description of POLCAL is given in the POLCAL User's Manual [9].

In the POLCAL technique the radar error model and corrections are done in three steps. The first step is phase calibration where the radar distortion matrices are assumed to be diagonal with only phase differences. That is, the measured scattering matrix is assumed to be

$$\boldsymbol{U} = \begin{bmatrix} s_{vv} & s_{vh}e^{i\phi_r} \\ s_{hv}e^{i\phi_t} & s_{hh}e^{i(\phi_r+\phi_t)} \end{bmatrix}.$$

where s_{pq} are the theoretical values for the scattering matrix elements. Reciprocity mandates that $s_{hv} = s_{vh}$ and, therefore, the quantity $u_{hv}u_{vh}^*$ must have a zero phase. By calculating the average phase of $u_{hv}u_{vh}^*$ over the image, the phase difference $\phi_t - \phi_r$ can be obtained. Then, by subtracting this phase difference from u_{hv}, a matrix $\boldsymbol{Z}$ is formed whose off-diagonal elements have almost identical phases. Next this matrix is symmetrized by the operation

$$\boldsymbol{Y} = \frac{1}{2}\left(\boldsymbol{Z} + \tilde{\boldsymbol{Z}}\right)$$

where $\tilde{\boldsymbol{Z}}$ is the transpose of $\boldsymbol{Z}$. The data is then coded and stored in the form of the Stokes scattering operator. To reduce the volume of data, as well as to reduce speckle, the Stokes scattering operator of groups of four adjacent pixels in a row are summed. To complete the phase calibration, the quantity $\phi_r + \phi_t$ is obtained from a trihedral response by calculating $Y_{hh}Y_{vv}^*$.

The next steps include cross-talk removal and adjusting for cochannel gain balance. Here the radar error model of the phase calibrated symmetrized response $(\boldsymbol{Y}')$ is represented by reciprocal transmit and receive distortion matrices, i.e.

$$\boldsymbol{Y}' = A\begin{bmatrix} 1 & \delta_2 \\ \delta_1 & f \end{bmatrix}\boldsymbol{S}\begin{bmatrix} 1 & \delta_1 \\ \delta_2 & f \end{bmatrix} \tag{22}$$

where $\boldsymbol{S}$ is the actual scattering matrix of the target, δ_1 and δ_2 represent the antenna cross-talk, and f is the cochannel imbalance. To correct for the cross-talk, two assumptions are made, (1) the magnitude of δ_1 and δ_2 are small compared to 1 and (2) the co- and cross-polarized terms of the scattering matrix of distributed targets are mutually uncorrelated, i.e.

$$\langle S_{hh}S_{hv}^* \rangle = 0, \qquad \langle S_{vv}S_{vh}^* \rangle = 0$$

where $\langle \cdot \rangle$ represents the ensemble average over a portion of the image that includes only natural targets. Using the above equations δ_1 and δ_2/f are found iteratively.

The phase of the cochannel imbalance f is calculated using the phase of VV and HH of the brightest pixel in the vicinity of the calibration target. The amplitude of f is obtained by calculating the ratio of the total power of VV to HH of a corner reflector response over 16×16 surrounding pixels. However, there is no clear justification as to why the HH and VV responses should be added noncoherently when finding f. And this is a general failing of POLCAL: It is presented as several transformations that make sense—that even give the right answers—but are rarely justified.

Finally, although the POLCAL technique intuitively makes sense, (22) must be viewed as an unjustified postulate. While (22) is of the same form as (1)—a well-accepted model for radar calibration—several steps in POLCAL are needed in order to transform $\boldsymbol{U}$ to $\boldsymbol{Y}'$. Applying these steps to (1) yields

$$g(\boldsymbol{U}) = g(\boldsymbol{RST})$$

where the function g represents the sum total of applying all these steps. Because the function g is so complicated—including the phase calibration, symmetrization, and four-look steps—it is not obvious that this reduces to:

$$\boldsymbol{Y}' = A\boldsymbol{R}'\boldsymbol{S}\tilde{\boldsymbol{R}}'$$

as is postulated in (22).

IV. Results and Comparison

This section presents results obtained by applying the two different calibration techniques described in Sections II.A, II.C, and III to the same scene. Each technique was applied twice, once with one of the trihedrals as the calibration target, and a second time with another trihedral as the calibration target. It should be mentioned here that the POLCAL technique is meant to use several trihedrals distributed along the range to account for variations of calibration parameters with range. Since the comparison made here does not use areas or targets at significantly different ranges, it was felt that POLCAL should be used with only one calibration target.

A. Data Formats and Test Scene

The results given in this section were obtained by processing the same JPL AirSAR scene as provided by JPL in two different formats. The format used by the techniques described in Section II is the so-called "hires" format, which provides the four scattering matrix elements as single-precision (four-byte) complex numbers in a grid measuring 4096×750. The format used by the POLCAL technique is radically different. The symmetrization, quantization from four bytes to one, and summing from one-look to four-look, as described in Section III, have been carried out to produce the so-called "compressed" format. Despite the use of different formats, the raw data used in their formation is identical, and so a comparison of the different techniques is valid.

Fig. 2 shows the total power image of the particular scene used during this study. The calibration targets were placed on a

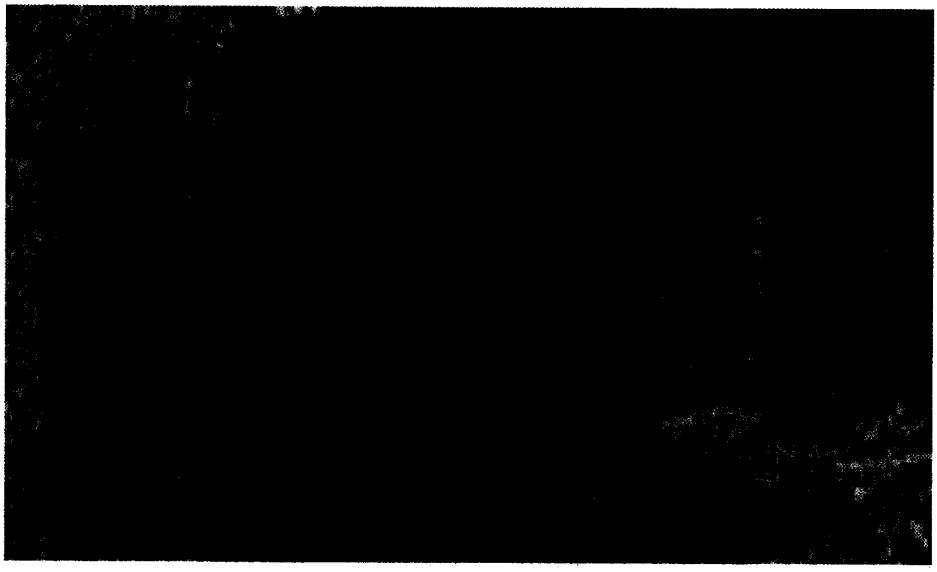

Fig. 2. Total Power image of calibration targets and surrounding area. Shown are all three trihedrals, the five PARC's, and the distributed target area to the left.

grassy plain, which was part of an airport near Pellston, MI, on April 1, 1990. Only L-band (24-cm wavelength) measurements were compared. Eight calibration targets are visible: three trihedrals (2.4 m on a side) in a vertical line, and five different Polarimetric Active Radar Calibrators (PARC's) in a horizontal line nearby. All targets were spaced about 60 m apart.

Fig. 3 shows the uncalibrated HH polarized raw data ("hires" format) in the vicinity of the three trihedrals. Note that the trihedrals are identical but that the responses are not: The trihedral at a range of 10 has much narrower tails in azimuth (± 3 pixels) than the other two (± 7 pixels, or more); there is also several dB difference (2.25 dB) in the peak values. This is of great concern since calibration depends on identical responses to identical targets. This will be addressed further in Section IV.D. One last thing to note about the responses in Fig. 3 is that the third trihedral has significant noise around it, due to some nearby brush. Because of this, the third trihedral response is contaminated and so was not used.

For both calibration procedures one of the remaining two trihedrals was used as the calibration target and the remaining point targets were used to assess the effectiveness of the calibration. Also, a distributed target was used for comparison despite the lack of any known values for its cross sections. This region is outlined in Fig. 2. It contains a random jumble of cut trees and low-growing brush.

B. Assessment of STCT Using Point Targets

Because STCT was developed for use with a single-antenna radar system, there is some doubt as to its applicability to the JPL AirSAR data which is obtained with a dual-antenna system. This section presents the results of applying this technique to the AirSAR data. The main figure of merit that is of interest in this section is the amount of cross-polarized response that is eliminated from the trihedral responses due to calibration. The general calibration method developed in II.B is assessed in IV.D.

To apply STCT, the central pixel of a trihedral response is used as the calibration target. This pixel is manually chosen as the center of the measured response with the spread due to the radar's ambiguity function. Fig. 4 shows the calibrated polarization signatures for one test trihedral with the other used as a calibration target. Note that a perfect trihedral would show no variation in the Ψ-direction, but otherwise would look similar to this figure. (See Table I for further data.) The results are excellent: The levels are within 1 dB of theory, with the cochannel imbalance being no more than 0.5 dB. Also, the cross-to-like isolation has improved from 20 dB before calibration to about 40 dB. The small discrepancies could be due to a number of factors. First, the ambiguity function is not the same for different calibration targets because they are not aligned perfectly with the SAR imaging grid. Second, because the calibration targets are assembled on-site from very large sheet-metal panels, any misalignment of the three sides can easily produce 1-dB differences in the different polarizations. Table I also shows the calibrated levels of two different PARC's: VV and 45°. The VV PARC signature is as expected with a large (23 dB as measured in chamber) isolation between VV and HH. The 45° PARC signature has the peak very nearly centered on $\chi = 0, \Psi = 45°$, as expected. Note that the variation in the backscattered power levels with different calibration trihedrals is due to the difference in measured peak power, which is due to different ambiguity functions.

This favorable comparison with the expected results leads one to conclude that this technique is applicable to the JPL AirSAR imaging radar data.

A. Assessment of POLCAL

Because the calibration trihedral is used only to determine

TABLE I
VALIDATION OF STCT

Cal. Target	Test Target	Backscattered Power Levels (dB)			
		hh	vv	hv	vh
Tri #1	Tri #2	32.72	32.19	-14.97	-12.12
Tri #2	Tri #1	34.66	35.19	-11.81	-8.97
Tri #1	VV PARC	-5.07	17.87	-8.92	-30.78
	45° PARC	16.88	14.61	16.10	15.75
Tri #2	VV PARC	-4.09	19.37	-6.98	-29.76
	45° PARC	17.85	16.10	17.21	17.10

The abbreviation "Tri" stands for trihedral. Theoretical results for a trihedral (test target) would be large numbers for the copolarized returns (hh and vv) while the cross-polarized returns (hv and vh) would be nonexistant (−dB).

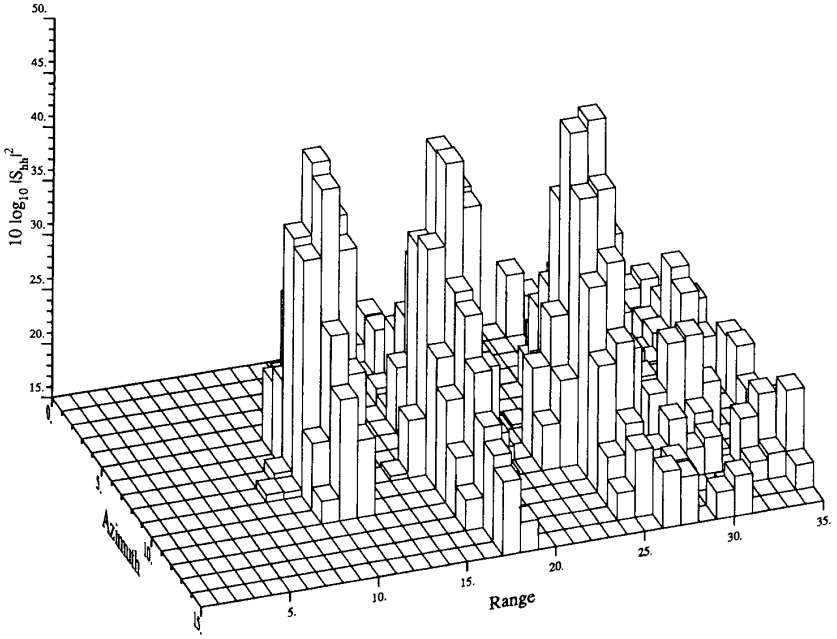

Fig. 3. Measured HH-polarized values in dB for all three trihedrals, in the "hires" format. A small region surrounding them is shown. Note that the response is significantly different in shape for the identical trihedrals: the trihedral at a range of 10 has much narrower tails in azimuth (±3 pixels) than the other two (±7 pixels, or more); there is also several dB difference (2.25 dB) in the peak values.

the cochannel imbalance and absolute level, this calibration technique gives noticeably different results when compared to those in Section IV.B. An added complication for point targets is that the levels cannot be compared until many adjacent pixels are used in the calculation of the signature. This is because POLCAL determines the absolute level through a summation of power in a region surrounding the calibration target. Table II gives the single-pixel powers of the two trihedrals after calibration with POLCAL. Here the cochannel imbalance is between 0.5 dB and 1 dB, slightly worse than for STCT. The cross-to-like isolation is generally 23 dB, 17 dB worse than for STCT, although, in one case, the isolation was 175 dB, apparently an unrepresentative coincidence since it appears only once.

To compare the absolute levels, the signatures are computed by summing over the same region that is used to sum the powers of the calibration target. The Stokes scattering operator [7] for each pixel in this region is summed. These results are given in Table II. Note that generally the signatures do not as closely resemble a trihedral as did those when using just a single pixel. The absolute levels, however, are within 1 dB of the expected levels.

Fig. 5 shows the 45° PARC, which looks quite different using the two different calibration schemes. The VV PARC has a 15-dB isolation, 8 dB worse than STCT, while the cross-pol signature is significantly distorted, apparently due to the conversion from high resolution format to compressed format. The 45° PARC now has **two** cross-pol peaks, at ±45°. This is due to the symmetrization step used in POLCAL.

B. Comparison Using a Distributed Target

The distributed target is a rectangular region 180 × 20 pixels

TABLE II
VALIDATION OF POLCAL

Cal. Target	Test Target	Backscattered Power Levels (dB)		
		hh	vv	hv and vh
Tri #1	Tri #1 (1 pixel)	29.52	30.21	5.85
	Tri #2 (1 pixel)	28.50	28.64	4.54
Tri #2	Tri #1 (1 pixel)	29.43	30.53	-145.57
	Tri #2 (1 pixel)	28.39	28.94	4.64
Tri #1	Tri #1 (summed)	33.83	33.84	9.00
	Tri #2 (summed)	33.94	33.58	10.80
Tri #2	Tri #1 (summed)	33.71	34.14	7.49
	Tri #2 (summed)	33.83	33.89	9.67
Tri #1	VV PARC (1 pixel)	6.80	21.64	-2.23
	45° PARC (1 pixel)	21.96	17.72	6.89
Tri #2	VV PARC (1 pixel)	6.80	21.95	-4.96
	45° PARC (1 pixel)	21.84	18.04	6.90

The abbreviation "Tri" stands for trihedral. Theoretical results for a trihedral (test target) would be large numbers for the copolarized returns (hh and vv) while the cross-polarized returns (hv and vh) would be nonexistant ($-\infty$dB). The notation "1 pixel" means that only the brightest pixel was used as the test target, whilt the notation "summed" means that many adjacent pixels were summed to yield the test target response.

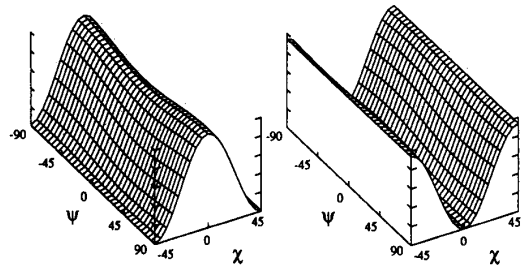

Fig. 4. Validation results for STCT. Shown is trihedral #2 when the calibration target was trihedral #1. Power values: hh = 32.72 dB, vv = 32.19 dB, hv = −14.77 dB, vh = 12.12 dB.

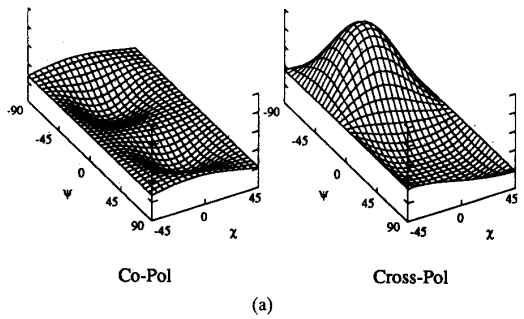

Fig. 5. Comparison of nonreciprocal target: STCT *vs.* POLCAL. Shown is the 45° PARC when the calibration target was trihedral #1. (a) is STCT. Power values: hh = 16.88 dB, vv = 14.61 dB, hv = 16.10 dB, vh = 15.75 dB. (b) is POLCAL. Power values: hh = 21.96 dB, vv = 17.72 dB, hv = 6.89 dB.The major difference is due to the symmetrization of the data in the compressed format for use by POLCAL.

in the hires format, and 45 × 20 pixels in the compressed format. This is a typical size for vegetation canopies with relatively uniform parameters. The region was chosen to be at nearly the same range as the calibration targets to avoid any problems associated with calibration parameter variability with range.

First, a comparison of the two formats, prior to calibration, is in order. Fig. 6 shows that the high resolution data has VV power of about 3.75 dB less than HH, while the compressed data has them 4.75 dB apart. Similar differences are observed between the high resolution and compressed formats ($\approx$ 0.4 dB) *after* calibration as well (Table III). Note that the HH-polarized return is higher for this scene. This is probably because that region is made up of many nearly horizontal tree trunks as a result of logging activities.

Because this is a distributed target, the calibration scheme described in Section II.C was used. The summation on D_{ij} was done over all pixels in the vicinity of the calibration target that had a cross-pol magnitude about 20 dB above the noise, as determined manually. A very important detail concerning this summation is the sign of the cross-talk factor, C. The sign of C is arbitrary, but in order to perform a valid summation, the sign of C used for each pixel must be consistent with all the other pixels. Essentially, this amounts to choosing the sign of C such that its phase is nearly the same for all pixels. With this done, the modified STCT calibration procedure gives the results in Table III. The signatures are very similar, the only difference being in their absolute levels—a difference of, at most, 0.75 dB. Hence, the differences in the measured

TABLE III
COMPARISON BETWEEN MODIFIED STCT AND POLCAL FOR A DISTRIBUTED TARGET

Cal. Method	Cal. Target	Data Format	Backscattered Power Levels (dB)			
			hh	vv	hv	vh
none	none	hi-resolution	14.71	10.96	7.00	7.25
		compressed	-3.31	-8.04	-11.40	
STCT	Tri #1	hi-resolution	-7.12	-10.95	-14.53	-15.17
	Tri #2	hi-resolution	-6.99	-10.60	-14.52	-14.71
POLCAL	Tri #1	compressed	-7.19	-11.29	-15.06	
	Tri #2	compressed	-7.31	-10.98	-14.96	

The abbreviation "Tri" stands for trihedral. The notation "STCT" for calibration method denotes the new algorithm presented here which is a modification of STCT for use in imaging SARS.

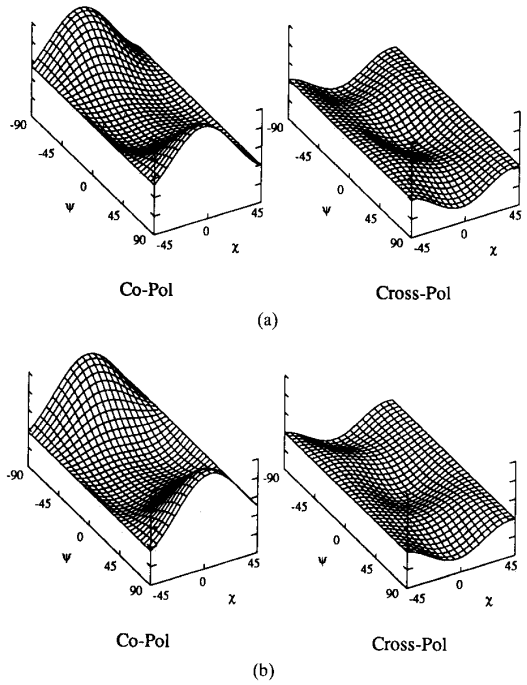

Fig. 6. Uncalibrated signature of distributed target region. (a) shows the high resolution format. Power values: hh = 14.71 dB, vv = 10.96 dB, hv = 7.00 dB, vh = 7.25 dB. (b) shows the compressed format. Power values: hh = –3.31 dB, vv = –8.04 dB, hv = –11.4 dB.

ambiguity function for the different calibration targets do not significantly affect the calibration of distributed targets. The results of the POLCAL scheme are very similar to the results of the STCT scheme as is shown in Table III. Also, note that the absolute levels are very similar. The difference between the two calibration schemes is less than 1 dB. This agreement gives us confidence that the calibration routines are performing well.

One other performance measure was used, at the suggestion of one of the reviewers. This involves a determination of the correlation of the cross-pol terms with the co-pol terms. After a successful calibration this correlation, as averaged over an area in the image, should be nearly zero for targets with azimuthal symmetry. The two measures taken were suitably normalized to account for the change of scale due to the absolute calibration:

$$\frac{\langle S_{hh}S_{hv}^{*}\rangle}{\langle S_{hh}\rangle\langle S_{hv}^{*}\rangle} \text{ and } \frac{\langle S_{hv}S_{vv}^{*}\rangle}{\langle S_{hv}\rangle\langle S_{vv}^{*}\rangle}.$$

The modified STCT technique presented in Section II showed improvements of 4.42 dB and 3.62 dB, while for POLCAL the improvements were 4.91 dB and 2 dB.

This condition is explicitly enforced in the formulation of the calibration method used in POLCAL, whereas in ours it is not used in the formulation. Both techniques show good improvements.

V. CONCLUSION

A new method for calibration of polarimetric imaging SAR's using point targets is developed. The technique requires a single calibration target, namely a trihedral, to find the ambiguity-distortion matrix (polarimetric ambiguity) function of the SAR system. In this method the radar error model is represented by the four-port network approach employed in the STCT. This error model is valid for polarimetric SAR's with both passive and active antenna array elements when the array elements are identical. An estimate for the backscattering coefficient is obtained by using the calibration matrix and assuming that the reflectivity of the terrain is constant over the pixels where the polarimetric ambiguity function is greater than some threshold above the noise level.

The validity of the technique is examined by calibrating a scene which includes a variety of point targets with known scattering matrices. It is found that the error model provided by the STCT is an appropriate one and enhances the measured polarization isolation of the point targets. The small discrepancies in the absolute values and polarization signatures are due to the fact that the point target response of a SAR depends on the relative position of the calibration target with respect to the center of the imaged pixel. Also the modified STCT technique is compared against the POLCAL technique for distributed targets and very good agreement is obtained. The POLCAL technique includes steps and approximations which are very different from the new technique. However, if the radar distortions are minimal (as here with the JPL AirSAR L-band radar) the POLCAL technique should provide satisfactory results.

ACKNOWLEDGMENT

The authors appreciate the help of the JPL Radar Science group in providing the POLCAL software and the AirSAR image data used in this study.

REFERENCES

[1] R. M. Barnes, "Polarimetric calibration using in-scene reflectors," Rep. TT.65, MIT, Lincoln Laboratory, Lexington, MA, Sept. 1986.
[2] L. J. Cutrona, "Synthetic aperture radar," in *Radar Handbook*, M. Skolnik, Ed. New York: McGraw-Hill, 1970.
[3] J. D. Klein, "Calibration of quadpolarization SAR data using backscattering statistics," presented at Proc. 1989 Intern. Geosci. Remote Sens. Symp., Vancouver, Canada, July 1989.
[4] K. Sarabandi, F. T. Ulaby, and M. A. Tassoudji, "Calibration of polarimetric radar systems with good polarization isolation," *IEEE Trans. Geosci. Remote Sensing*, vol. 28, Jan. 1990.
[5] K. Sarabandi and F. T. Ulaby, "A convenient technique for polarimetric calibration of single-antenna radar systems," *IEEE Trans. Geosci. Remote Sensing*, vol. 28, Nov. 1990.
[6] D. R. Sheen and E. S. Kasischke,"Comparison of SAR polarimetric calibration technique using clutter," presented at Proc. 1989 Intern. Geosci. Remote Sens. Symp., Vancouver, Canada, July 1989.
[7] F. T. Ulaby and C. Elachi, Eds., *Radar Polarimetry for Geoscience Applications*. Artech, 1990.
[8] J. J. van Zyl, " Calibration of polarimetric radar images using only image parameters and trihedral corner reflector responses," *IEEE Trans. Geosci. Remote Sensing*, vol. 28, May 1990.
[9] J. J. van Zyl, C. F. Burnette, H. A. Zebker, A. Freeman, and J. Holt, "POLCAL User's Manual," Jet Propulsion Laboratory, Aug. 1990.
[10] M. W. Whitt, F. T. Ulaby, P. Polatin, and V. V. Liepa, "A general polarimetric radar calibration technique," *IEEE Trans. Antennas Propagat.*, vol. 39, Jan. 1991.
[11] H. A. Zebker and Y. Lou, "Phase calibration of imaging radar polarimeter Stokes matrices," *IEEE Trans. Geosci. Remote Sensing*, vol. 28, Mar. 1990.
[12] A. L. Gray, P. W. Vachon, C. E. Livingston, and T. I. Lukowski, "Synthetic aperture radar calibration using reference reflectors," *IEEE Trans. Geosci. Remote Sensing*, vol. 28, May 1990.

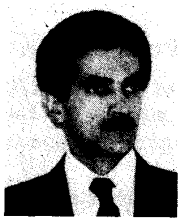

Kamal Sarabandi (S'87–M'90) was born in Tehran, Iran, on November 4, 1956. He received the B.S. degree in electrical engineering from Sharif University of Technology, Tehran, in 1980. He received the M.S.E. degree in electrical engineering in 1986, and the M.S. degree in mathematics and the Ph.D. degree in electrical engineering in 1989, all from the University of Michigan.

From 1980 to 1984 he worked as a microwave engineer in the Telecommunication Research Center in Iran. He is presently an assistant research scientist in the Department of Electrical Engineering and Computer Science at the University of Michigan. His research interests include electromagnetic scattering, microwave remote sensing, and calibration of polarimetric SAR systems.

Dr. Sarabandi is a member of the Electromagnetics Academy and USNC/URSI Commission F.

Leland Pierce (S'85–M'85–M'87) received the B.S. degrees in electrical engineering and aerospace engineering in 1983, and both the M.S. and Ph.D. degrees in electrical engineering, in 1986 and 1991, respectively, all from the University of Michigan, Ann Arbor.

Since then he has been the head of the newly formed Microwave Image Processing Facility within the Radiation Laboratory in the Electrical Engineering and Computer Science Department at the University of Michigan. He is responsible for research into the uses of Polarimetric SAR systems for remote sensing applications, specifically, forest canopy parameter inversion.

Fawwaz T. Ulaby (M'68–SM'74–F'80) received the B.S. degree in physics from the American University of Beirut, Lebanon, in 1964, and the M.S.E.E. and Ph.D. degrees in electrical engineering from the University of Texas, Austin, in 1966 and 1968, respectively.

He is currently Professor of Electrical Engineering and Computer Science at the University of Michigan, Ann Arbor, and Director of the NASA Center for Space Terahertz Technology. His interests include microwave and millimeter wave remote sensing, radar systems, and radio wave propagation. He has authored several books and published over 400 papers and reports on these subjects.

Dr. Ulaby is the recipient of numerous awards, including the IEEE Geoscience and Remote Sensing Distinguished Achievement award in 1983, The IEEE Centennial Medal in 1984, and the Kuwait Prize in applied science in 1986.